Available online at www.sciencedirect.com
SCIENCE DIRECT
Journal of Catalysis 230 (2005) 28–37
JOURNAL OF CATALYSIS
www.elsevier.com/locate/jcat

Conversion of xylene over mordenites: an operando infrared spectroscopy study of the effect of Na^+

Olivier Marie [a,*], Frédéric Thibault-Starzyk [a], Pascale Massiani [b]

[a] *Laboratoire Catalyse & Spectrochimie, CNRS-ENSICAEN, 6 Bd du Maréchal Juin, 14050 Caen cedex, France*
[b] *Laboratoire de Réactivité de Surface, CNRS-UPMC, 4 place Jussieu, casier 178, 75252 Paris cedex 05, France*

Received 5 August 2004; revised 21 September 2004; accepted 23 September 2004

Available online 28 December 2004

Abstract

A series of progressively proton-exchanged sodium mordenite samples was studied by operando infrared spectroscopy during xylene conversion. This unique, powerful tool allowed us to characterize the species adsorbed to the surface during catalysis and to follow the evolution of the active sites as the reaction proceeded. We were then able to correlate the surface data with the catalytic results obtained by gas-phase chromatography analysis. When very few hydroxyls are present on site O_7H close to the main-channel walls, the initial isomerization selectivity is very high and the high Na^+ content leads to the preferential adsorption of 1,2,4-TMB inside the micropores. When the amount of acidic hydroxyls increases, new sites O_2H are generated at the intersection between main channels and side pockets. The initial disproportionation selectivity then increases roughly. Finally, the last hydroxyls appear on site O_9H located at the end of the side pockets. These constrained hydroxyls are not accessible to the reactant in the reaction conditions, but their presence leads to a global activity increase without any selectivity modification. Acid strength considerations, together with the observation of the "working hydroxyls," indicate an indirect effect of O_9H on the overall activity, which is probably related to a modification in the void space inside the micropores.

Keywords: Catalysis; Xylene; Isomerization; Disproportionation; Zeolite; Mordenite; Operando; FTIR spectroscopy

1. Introduction

Mordenite is an important zeolite, used in many industrial processes, particularly in petrochemistry and refining. It has the strong acidity necessary for paraffin isomerization [1]. For cumene synthesis, it is used after adjustment of its meso/micropore system by controlled dealumination [2]. It is also used for the isomerization of C_8 aromatic fraction, the acidity of which must be adjusted by partial cation exchange [3,4]. In the latter case, the role of the cation is not yet completely clear.

Two main reactions can take place during xylene conversion (Scheme 1): isomerization, which is used to increase the relative amount of highly valued *p*-xylene, and disproportionation, which leads to toluene and trimethylbenzene (TMB) in equal amounts. It is now well established that isomerization involves a monomolecular mechanism [5], whereas disproportionation occurs through a bimolecular mechanism in which formation of the bulky diaryl methane intermediate can be inhibited by steric constraints. Thus, *m*-xylene conversion was proposed as a test reaction to distinguish the presence or absence of 12-member ring channels inside zeolites [6]. Moreover, it was shown that the two reactions do not take place on the same types of acidic sites on mordenite [4]; disproportionation requires more acidic sites than isomerization [7].

However, until recently, the location and strength of the various Brønsted acid sites in mordenite remained a matter of debate. Initial studies, based mostly on FTIR data, proposed the presence of two main acidic OH types, located inside main channels and side pockets, respectively. Calorimetric measurements of the adsorption of ammonia

* Corresponding author. Fax: +33 231 452 822.
E-mail addresses: marieo@ismra.fr (O. Marie), fts@ismra.fr (F. Thibault-Starzyk), massiani@ccr.jussieu.fr (P. Massiani).

0021-9517/$ – see front matter
doi:10.1016/j.jcat.2004.09.023

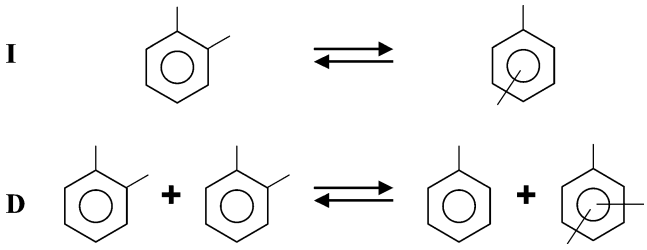

Scheme 1. The two main ways for *o*-xylene conversion over acidic catalysts: (**I**) isomerization, which gives *m*-xylene and *p*-xylene, and (**D**) disproportionation which gives toluene and trimethylbenzene (TMB).

suggested that the OH types in the side pockets are stronger than in the main channels [7], but these data happened to be strongly biased by confinement effects [8]. FTIR studies of CO and N_2 adsorption at low temperature, on the other hand, showed that stronger sites are located in the main channels, where they are less constrained [9,10]. Disproportionation is indeed favored by the presence of strong acid sites, but is surprisingly suppressed when less acidic but confined sites in the side pockets are removed by controlled cation exchange [3].

In a recent paper, we described the influence of progressive Na^+/H^+ exchange on the number and location of OH groups in mordenite [11]. In agreement with recent proposals [12,13], we showed that not only two but at least three different locations for Brønsted sites can be clearly distinguished in mordenite: one constrained O_9H site inside the side pockets of the structure (denoted here as OH_{const}) and two unconstrained sites (denoted as $OH_{unconst}$) in the main channel (O_7H) and in an intermediate location (O_2H) at the opening of the side pocket. Our series of catalysts had been obtained by progressive exchange of the sodium form of the zeolite toward the acidic form. During the exchange process, sodium cations were first replaced by protons in the main channels, the intermediate sites were exchanged next, and the last sodium ions remained in the side pockets. We had thus a series of catalysts in which we controlled the location of Brønsted sites in the three possible sites. In the present work, we used the same series of catalysts for an operando study of xylene conversion. We established the relationships, during reaction, between adsorbed surface species, perturbation of each acid site (identified by FTIR spectroscopy), and catalytic performance of the solids (identified by gas chromatography). We can thus explain the influence of cations and of the three acid sites on the catalytic selectivity.

2. Experimental

Various mordenite samples with varying H^+ and Na^+ cationic contents were obtained by exchange of a parent sodium mordenite sample (from Tosoh Corp.; Si/Al = 10.2) in a NH_4Cl solution (0.1 N), followed by a mild thermal treatment at 723 K (decomposition of the NH_4^+ ions into NH_3 and H^+) performed in flowing N_2 (physicochemical characterizations) or in a vacuum. Table 1 details the conditions of the NH_4^+ exchange and the chemical contents (Na/Al and Si/Al atomic ratios) for all of the thermally activated H_xNa_{100-x}MOR samples, where x and $100-x$ are the percentages of H^+ and Na^+ cations, respectively. Note that x is also the level of exchange (in %) of protons for Na^+ cations. The quantification and the determination of the distribution of the Brønsted acid sites was obtained from the adsorption of various probe molecules as detailed in Ref. [11]. The thermal treatment was gentle enough (heating slower than 1 K min^{-1}) to ensure the absence of measurable framework dealumination as checked by ^{27}Al MAS NMR and FTIR spectroscopies [11]. In agreement, no acid Lewis sites were detected by pyridine adsorption.

Nitrogen adsorption isotherms at 77 K were obtained with a Micromeritics ASAP 2400 apparatus (all samples were treated under a vacuum at 700 K before measurements) and used for the determination of microporous volumes according to the Langmuir model

$$\frac{V_{ads}}{V_m} = \frac{Kx}{1+Kx},$$

where V_{ads} stands for the nitrogen volume adsorbed under the equilibrium pressure P, V_m stands for the microporous volume, K stands for the adsorption equilibrium constant, and $x = P/P^\circ$ stands for the relative pressure. The linearization of this law for relative pressure in the range $0.05 < x < 0.2$ led to the microporous volumes reported in Table 1. The presence on the isotherm of a hysteresis loop between the adsorption and desorption branches (which are horizontal and parallel over a wide pressure range) indicates

Table 1
Physicochemical characterization of the H_xNa_{100-x} samples

Sample name	NH_4Cl (0.1 N)/H_0Na_{100}MOR (weight/weight)	Na/Al ratio (mol/mol)	Si/Al ratio (mol/mol)	$H^+ = (Al–Na^+)$ (μmol g_{cat}^{-1})	$V_{microporous}$ (cm^3 g_{cat}^{-1})
H_0Na_{100}MOR	–	1	10.2	0	0.193
$H_{13}Na_{87}$MOR	2.5	0.87	10.8	160	n.d
$H_{24}Na_{76}$MOR	4.0	0.76	12.9	250	n.d
$H_{31}Na_{69}$MOR	3.5	0.69	10.2	400	n.d
$H_{61}Na_{39}$MOR	7.0	0.39	10.2	800	n.d
$H_{72}Na_{28}$MOR	9.5	0.28	10.3	930	0.198
$H_{93}Na_7$MOR	50	0.07	10.6	1190	n.d
$H_{100}Na_0$MOR	75 (repeated 3 times)	0.007	10.4	1290	0.215

a wide distribution of meso and/or macropores that is identical for all of the samples and is estimated to be 0.05 $cm^3\ g^{-1}$.

Conversion of *o*-xylene was performed at 573–623 K, at atmospheric pressure, and under flow conditions, with weight space velocities in the range of 4–60 h^{-1}. Analysis of the reaction products was performed with a Delsi DI 200 gas chromatograph equipped with a SGE BP 20 column permitting meta and para xylene isomer separation. A multiposition valve actuator (VICI) containing eight loops was used to take and store samples at determined times or to make direct online analysis. All organic compounds (reactants and products for chromatograph calibration) were 99% pure (Aldrich).

Infrared spectra were recorded with a Nicolet Magna 550 FTIR spectrometer, in a quartz infrared cell connected to a vacuum line for experiments conducted at room temperature, and in a reactor cell already described [14] for operando spectroscopy at reaction temperature. The decomposition of the ν(OH) bands at high temperature was done with Grams/386 software (V1.04, Galactic Industries Corp., 1996), with a procedure adapted from that of Makarova [15]. To take into account the influence of temperature, initial values for the fitting were modified as follows. Frequency values were lowered by 18 cm^{-1} compared with room temperature, and bands were broadened to 35 and 18 cm^{-1} for the high-frequency and low-frequency components, respectively.

3. Results and discussion

An operando study is the study of a working catalyst, for which catalytic activity and selectivities are measured, while at the same time the adsorbed species on the catalyst surface ares monitored [16]. The first step for such an approach is to identify the spectra of possible surface species, reactants or products, under reaction conditions. The last step is to correlate catalytic data with the perturbation of the surface to determine the selective active sites and eventually the reaction mechanisms.

3.1. Spectral identification of surface species

o-Xylene conversion was first performed in a traditional fixed-bed catalytic reactor without infrared monitoring to identify possible products by gas chromatography. In agreement with Scheme 1, the products obtained were *m*- and *p*-xylene, created by isomerization, and toluene and trimethylbenzene (1,2,4-, 1,3,5-, and 1,2,3-TMB), formed by disproportionation. Only light traces of products from cracking were sometimes detected.

The infrared spectra of each of these species were recorded in the gas phase, and after adsorption on $H_{100}Na_0$MOR (at room temperature to avoid any reaction) and on H_0Na_{100}MOR (at room temperature and at 623 K). The infrared bands typical of the various products adsorbed on acidic OH groups and on Na^+ cations are reported in Table 2. The frequencies for ν(CH) vibration bands are all in a very short range, and these bands cannot be used for identification purposes. Rather, products can be identified by analysis of the ν_{19b}(C=C) bands, which, for instance, appear in the case of adsorption at 298 K on acidic hydroxyls as fine and intense singlets centered at 1495 cm^{-1} for toluene, 1505 cm^{-1} for 1,2,4-TMB, and 1515 cm^{-1} for *p*-xylene. The ν_8(C=C) vibrations of aromatic rings are more significantly shifted to lower wavenumbers upon adsorption on cations than when adsorption takes place by H-bond, because of the strong affinity between aromatic rings and alkaline cations [17,18]. The $\delta(CH_3)$ vibration bands (δ_{as} around 1450 cm^{-1} and δ_s around 1380 cm^{-1}) are also sensitive to the adsorption mode, but not enough to be of any use to us.

Finally, to study the temperature effect on the vibration bands and to get closer to the reaction conditions, we undertook our experiment over H_0Na_{100}MOR at 623 K under flow conditions. No reaction took place because of the absence of Brønsted acid sites, and thus we were able to obtain the infrared fingerprint of each product interacting with Na^+ under reaction conditions. Fig. 1 shows the spectra obtained after 1 min on stream at constant space velocities (whsv = 15 h^{-1}) for each *o*-xylene conversion product. The ν(CH) vibration region (2800–3100 cm^{-1}) indicates that *o*-xylene and 1,2,4-TMB give rise to the most intense bands, which suggests an initial higher amount of adsorbed species if we consider that the ν(CH) extinction coefficient varies very little from toluene to TMB, which possess the same aromatic nature and methyl groups. The right part of Fig. 1 shows an enlargement in the ν(C=C) and δ(CH) vibration region. Each peak is pointed, and wavenumbers are summarized in Table 2 together with their attributions. It is obvious from the comparison of adsorption over H_0Na_{100}MOR at 298 K and 623 K that the ν_8(C=C) vibration shifts toward the lower wavenumbers with increasing temperature. The shift magnitude nevertheless depends on the product: from 4 cm^{-1} for 1,2,3-TMB to 11 cm^{-1} for *m*-xylene. This general trend is expected from thermal effects, and both the aromatic ring vibrations ν_{19a} and ν_{19b} undergo the same qualitative effect. In addition, the separation between the ν_{19b} peaks relative to the three easily identified products (toluene, 1,2,4-TMB, and *p*-xylene) is less important at 623 K, so that quantitative measurements will be more difficult under reaction conditions where a mixture of products is present.

3.2. Accessibility of sites

The adsorption of each species from a nitrogen flow (adjusted to maintain constant partial pressure and contact time) at 623 K on H_0Na_{100}MOR was monitored by infrared spectroscopy over time until saturation. The comparative determinations of adsorbed quantities were made with a chosen band for each of the species and the corresponding gas phase extinction coefficients (previously measured from known pressure). The absolute value of adsorbed amounts was not

Table 2
Summary of the wavenumbers (in cm^{-1}) for the main vibrations of the products obtained during xylene conversion

Aromatic species		*o*-Xylene	*m*-Xylene	*p*-Xylene	Toluene	1,2,4-TMB	1,3,5-TMB	1,2,3-TMB
ν(CH) aromatic	Gas phase	3067	–	3056	3072	3050	–	3051
	OH (298 K)	–	–	–	–	–	n.d.	n.d.
	Na^+ (298 K)	3066–3048	–	–	3061	–	–	–
	Na^+ (623 K)	3058	–	–	3054	–	–	3050
ν(CH) aromatic	Gas phase	3030	3030	3027	3037	3015–2978	3024	–
	OH (298 K)	–	3027	–	3031	3002–2979	n.d.	n.d.
	Na^+ (298 K)	2994	3030	3025	3026	3021–2989	–	2970
	Na^+ (623 K)	3014	3027	3015	3017	3019	3019	–
ν(CH) methyl group	Gas phase	2937	2935	2934	2936	2936	2932	2952
	OH (298 K)	2944–2925	2927	2929	2924	2941–2926	n.d.	n.d.
	Na^+ (298 K)	2945–2925	2957–2926	2956–2928	2925	2946–2926	2962–2928	2940–2925
	Na^+ (623 K)	2945–2926	2924	2924	2924	2945–2925	2937–2915	2928
ν(CH) methyl group	Gas phase	2883	2879	2880	2886	2880	2876	2878
	OH (298 K)	2877–2865	2867	2872	2876	2867	n.d.	n.d.
	Na^+ (298 K)	2870	2867	2872	2870	2868	2859–2820	2871
	Na^+ (623 K)	2874	2870	2870	2870	2868	2862	2860
ν_8 (C=C) aromatic ring	Gas phase	1604	1613	–	1609	1616	1612	1594
	OH (298 K)	1604	1607	–	1601	1615	n.d.	n.d.
	Na^+ (298 K)	1597	1602	–	1596	1609	1602	1582
	Na^+ (623 K)	1591	1591	–	1586	1603	1594	1578
ν_{19b} (C=C) aromatic ring	Gas phase	1494	1498	**1520**	**1500**	**1508**	–	1478
	OH (298 K)	1496–1488	1485	**1515**	**1495**	**1505**	n.d.	n.d.
	Na^+ (298 K)	1499–1487	1484	**1511**	**1494**	1507–**1499**	–	1472
	Na^+ (623 K)	1482	1478	**1504**	**1489**	**1496**	–	1460
ν_{19a} (C=C) aromatic ring and/or $\delta(CH)_{as}$ methyl group	Gas phase	1466	1449	1432	1462	1460	1460	1450
	OH (298 K)	1466–1455	1465	1458–1449	1464–1452	1454	n.d.	n.d.
	Na^+ (298 K)	1464–1446	1464	1459–1449	1466–1448	1455	1463	1446
	Na^+ (623 K)	1462	–	–	1445	1459–1453	1461	–
$\delta(CH)_s$ methyl group	Gas phase	1388	1384	1384	1384	1384	1385	1389
	OH (298 K)	1387	1382	1383	1383	1385	n.d.	n.d.
	Na^+ (298 K)	1389	1385	1387	1386	1388	1386	1393–1387
	Na^+ (623 K)	1391	1385	1387	1387	1390	1387	1390

Values are given for the gas phase and for the adsorbed state onto $H_{100}Na_0$MOR at 298 K and onto H_0Na_{100}MOR at 298 K and 623 K. n.d. stands for 'not determined' whereas (–) means that no vibration was observed.

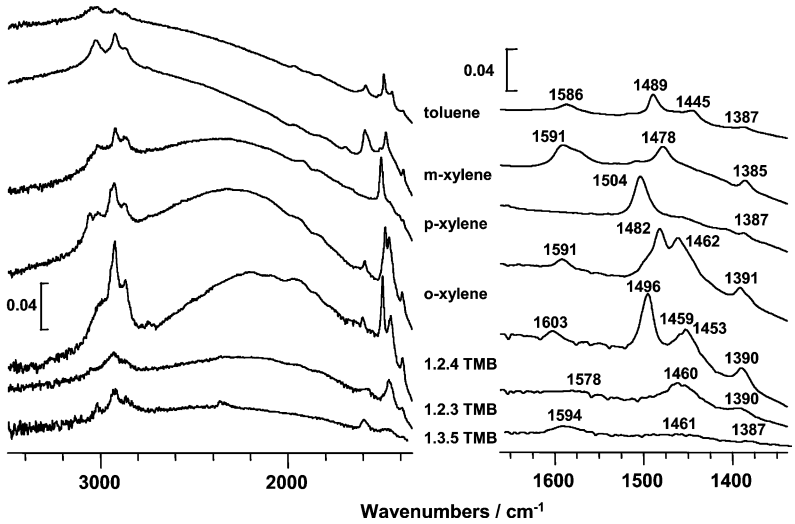

Fig. 1. Infrared spectra for each xylene conversion product adsorbed alone over H_0Na_{100}MOR sample at 623 K. Free H_0Na_{100}MOR spectrum was subtracted for clarity.

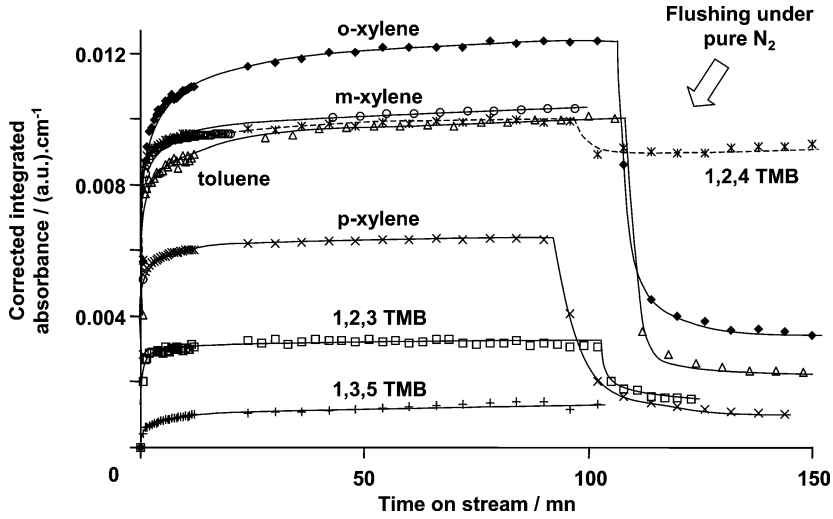

Fig. 2. Evolution of the amount of adsorbed species with time on stream (pure product diluted in N_2 at WHSV = 15 h^{-1}) at 623 K over H_0Na_{100}MOR (calculated from the corrected intensities of typical infrared bands).

Table 3
Fraction of perturbated hydroxyls infrared absorbance upon adsorption of the main products of xylene conversion at 298 K (first line) and percentages of accessible hydroxyls when considering (*) the whole hydroxyls and (**) only unconstrained hydroxyls (calculated from integrated area of infrared bands)

Product	*o*-Xylene	*m*-Xylene	*p*-Xylene	Toluene	1,2,4-TMB
$\Delta A_{OH}/A_{OH}$	39%	41%	46%	49%	41%
$^{*}\Delta n_{OH}/n_{OH\ total}$	[44–46%]	[46–48%]	[52–54%]	[55–57%]	[46–48%]
$^{**}\Delta n_{OH\ unconst}/n_{OH\ unconst}$	[59–69%]	[62–72%]	[69–81%]	[74–86%]	[62–72%]

accessible, but we obtained meaningful relative quantities, assuming that the variation of the extinction coefficient from the gas phase to the adsorbed phase is the same for all compounds. The evolutions with time on stream of the relative amounts adsorbed for all products (Fig. 2) show that *o*-xylene is the most easily adsorbed. Toluene, *m*-xylene, and 1,2,4-TMB have the same adsorption capacity, but the kinetics for toluene adsorption is slower. As pure nitrogen is passed over the surface, 1,2,4-TMB remains strongly adsorbed, because of its strong interaction with Na^+ ions. The two other TMBs are not adsorbed in large amounts on mordenite because of their large molecular diameter.

On the acidic sample, the study of adsorption was not possible under the same conditions because the reaction started at temperatures above 473 K. It was therefore performed at 298 K in the classical quartz in situ cell. At that temperature, the terminal silanol groups give an infrared band at ca. 3745 cm^{-1}, whereas the ν(OH) vibration band for acidic OH groups in mordenite has three components [11,19]: the high-frequency component (3610 cm^{-1}) is assigned to unconstrained acidic hydroxyls corresponding to sites O_7H in the main channels of the porous structure; the low-frequency component (3595 cm^{-1}) is assigned to constrained acidic O_9H groups in the side pockets; the intermediate component is due to unconstrained protons in sites O_2H, located at the opening of the side pocket and pointing in the main channels. Upon adsorption (T = 298 K, $P_{equilibrium}$ = 3 mbar), the interaction takes place through hydrogen bonding with acidic hydroxyls (3610–3605 cm^{-1}) and terminal silanols. To characterize only the interaction with acidic hydroxyls, we corrected all of the spectra from the specific hydrogen bonding with terminal silanols. The spectra obtained after each product adsorption over H_0Na_{100}MOR at 298 K presented not only bands due to an interaction with Na^+ cations but also bands due to an interaction through hydrogen bonding with silanols. These last spectra were thus used for correction, and we managed to isolate the specific interaction of each product with the acidic hydroxyls of $H_{100}Na_0$MOR. For every adsorbed compound, the OH_{const} were unperturbed at 298 K, confirming the strongly restricted access to side pockets at that temperature. We have to stress that OH_{const} remain out of reach of aromatic molecules only if the zeolitic structure is perfectly preserved. Access to the side pockets can be strongly modified by thermal treatment, for example, if the heating is faster than 1 K min^{-1} [20].

The percentage of Brønsted acid sites accessible to each product was then obtained from the ratio between the integrated absorbances of interacting hydroxyls at equilibrium and free hydroxyls before any adsorption. The first line ($\Delta A_{OH}/A_{OH}$) in Table 3 illustrates the "gross" value obtained when the nature of the interacting hydroxyls is not taken into account. If we consider that the wavenumber of interacting hydroxyls (3610–3605 cm^{-1}) is typical for un-

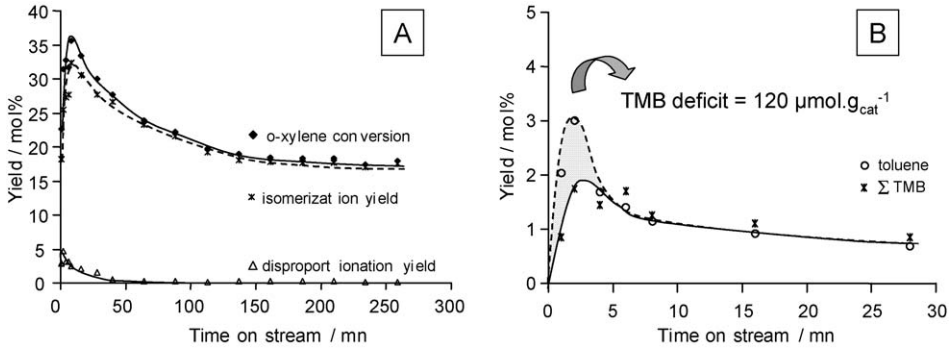

Fig. 3. Reaction of *o*-xylene over $H_{24}Na_{76}$MOR at 623 K and WHSV = 15 h^{-1}. (A) Evolution of xylene conversion, and isomerization and disproportionation yields with time on stream. (B) Comparison between toluene and TMB yields (outlet gas products measured by gas chromatography).

constrained hydroxyls [11], we need to correct this value, taking into consideration both the partition of the whole hydroxyls on their various sites and their respective extinction coefficients. For this purpose, as was described in the Introduction, sites O_7H close to the main channel walls and O_2H sites at the intersection between main channels and side pockets can be grouped as unconstrained hydroxyls ($OH_{unconst}$). Their population was allowed to vary between 2/3 and 3/4 of the overall hydroxyl amount according to Ref. [11]. The last OH_{const} located at the end of the side pockets were given an extinction coefficient $\varepsilon(OH_{const})$ such as $\varepsilon(OH_{const}) = 1.52\varepsilon(OH_{unconst})$, as was proposed by Makarova et al. [15]. The amounts of perturbed OH were then estimated from mathematical treatment of the quantitative data; the results are summarized in Table 3, including the percentages of OH interacting upon adsorption for the fraction of the whole heterogeneous OH groups (second line) and for the fraction of the accessible $OH_{unconst}$ groups (third line). According to their molecular dimensions, compounds such as *o*-xylene, *m*-xylene, and 1,2,4-TMB offer access to the lowest part of acidic hydroxyls (around 46% of the overall amount). When the kinetic diameters of the compounds decrease (*p*-xylene and toluene), their accessibility to Brønsted acid sites increases, but the whole unconstrained hydroxyl is never consumed (only 86% is the maximum value for toluene). We must conclude that from both qualitative and quantitative considerations, the OH_{const} acidic sites located at the end of the side pockets are not accessible at 298 K to the products engaged in *o*-xylene conversion. Moreover, we have to report a different ranking for adsorption capacity over H_0Na_{100}MOR at 623 K (*o*-xylene as the main adsorbed product on Na^+) and $H_{100}Na_0$MOR at 298 K (toluene as the main product interacting with hydroxyls). Finally, we would like to note that it was not possible to compare the adsorption capacities in one specific product for the two extreme samples of our series because the experimental conditions were not comparable; nevertheless as the total microporous volume increases with the replacement of Na^+ cations by acidic hydroxyls (Table 1), we would expect an increasing adsorption capacity with the hydroxyl amount at least for the smallest molecules, such as toluene.

3.3. Operando study

Sample $H_{24}Na_{76}$MOR contains only a small amount of Brønsted sites, and its catalytic activity is low. We used it to simplify the operando approach by working at low conversion to limit coke formation. Fig. 3A shows the conversion of *o*-xylene at 623 K and the corresponding yields measured by GC. The conversion goes through a maximum (∼ 35%) after the first minutes (induction period) and rapidly stabilizes at half of that value. The yield of isomerization displays the same behavior, whereas the yield of disproportionation (calculated from toluene + TMBs) is initially low (∼ 5%) and falls to zero rapidly, although disproportionation is the main thermodynamic path, as it can be calculated from thermodynamics tables [21]. The low selectivity for disproportionation can be explained by steric constrains and kinetic limitations (the activation energy is higher for disproportionation than for isomerization [22]). Some other authors, working at higher space velocity (200 h^{-1}), did not observe the induction period [23]. Such a phenomenon was reported, however, in the case of di-ethyl-benzene disproportionation on H–Y zeolite [24]. The induction period was then due to a default of di-ethyl-benzene in the gas phase, which the authors explained by the time needed to reach adsorption equilibrium between reactants and products [25]. In our experiment, we do observe a default in gaseous total TMB amount (by GC) during the induction period, compared with the amount of toluene produced (Fig. 3B); the expected values are theoretically identical. Integrating the amount over time on stream, we determined a default of 120 µmol TMB per gram of catalyst ($H_{24}Na_{76}$MOR), which is compatible with the adsorption capacity (750 µmol pyridine per gram of $H_{100}Na_0$MOR [11]). The induction period is thus due to a fast initial adsorption of TMB on the catalyst.

Fig. 4A reports the main infrared spectra for adsorbed species at selected reaction times. Very few data are available in the literature concerning adsorption equilibrium under reaction conditions. *o*-Xylene is obviously the major component of the gas phase in the reactor at the beginning of the reaction, because the conversion is then very low (22% after 1 min on stream). In agreement with the results in Table 2, we therefore assign to *o*-xylene the infrared band visible

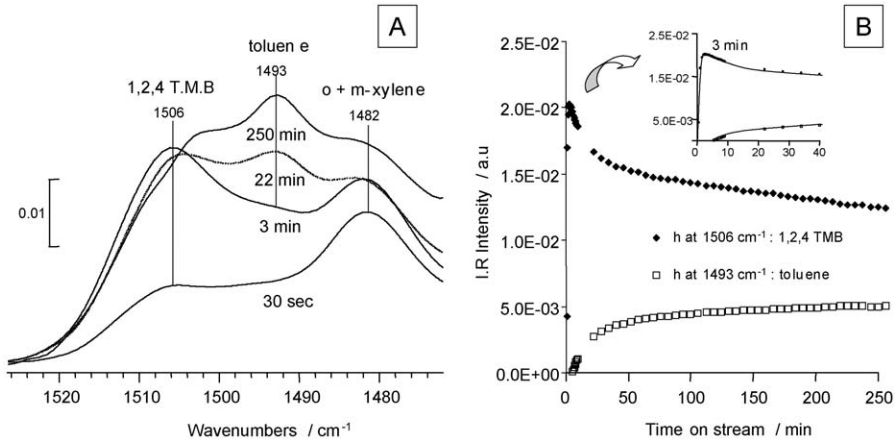

Fig. 4. Infrared spectra (ν_{19b} vibration) of adsorbed species after selected times on stream (A) and evolution of the infrared intensities relative to adsorbed toluene and 1,2,4-TMB with time on stream (B) during *o*-xylene conversion over $H_{24}Na_{76}$MOR at 623 K and WHSV = 15 h^{-1}.

at 1482 cm^{-1} after 30 s of reaction (Fig. 4A). After a few minutes, a band at 1506 cm^{-1} becomes the main feature in the spectrum. Assigning this band to the *p*-xylene ν_{19b} vibration, as would be suggested by our results at reaction temperature on the sodium sample (Table 2), seems impossible since *p*-xylene is a secondary product that can only be formed by isomerization of *m*-xylene, itself obtained from *o*-xylene [5]

o-xylene ⇆ *m*-xylene ⇆ *p*-xylene.

There has been a bimolecular mechanism reported recently for isomerization by transalkylation between xylene and disproportionation products [22,26], but this reaction can take place only in large pores, after disproportionation reaches a high yield, and it can probably be ruled out here. We therefore assigned the 1506 cm^{-1} band to 1,2,4-TMB, which led to a band at 1496 cm^{-1} when 1,2,4-TMB was adsorbed on H_0Na_{100}MOR. As we already mentioned, 1,2,4-TMB is quickly adsorbed in significant amounts on our samples (Fig. 2). Moreover, the di-aryl-methane intermediate to the formation of 1,2,4-TMB is preferentially stabilized in mordenites [6], and 1,2,4-TMB is then favored among TMB isomers in this zeolite by both thermodynamics and structural considerations. At the end of the reaction, a last infrared component appears at 1493 cm^{-1}, which we assign to the ν_{19b} vibration in toluene (it was at 1489 cm^{-1} on H_0Na_{100}MOR). The *m*-xylene isomer is probably also present and contributes to the intensity of the *o*-xylene band at 1482 cm^{-1}, but *p*-xylene is never detected on the surface. The differences in frequencies between these and those on H_0Na_{100}MOR are certainly due to the simultaneous presence of acidic OH groups and Na^+ ions. Finally, as we expected, no coke deposit was observed on this high-sodium sample at low conversion, as indicated by the absence of the typical infrared coke bands around 1585 and 1354 cm^{-1} [27].

The evolution with time of the amount of adsorbed 1,2,4-TMB as deduced from quantitative infrared analysis (1506 cm^{-1} band) is shown in Fig. 4B. This amount clearly increases during the induction period, and it decreases later on, when a significant amount of toluene builds up on the surface. The model we propose, to take these observations into account, is based on a competitive adsorption of reactants and products. In a first step, *o*-xylene adsorbed to $H_{24}Na_{76}$MOR is transformed into three main products: (i) *m*-xylene, which contributes to the same band at 1482 cm^{-1} as *o*-xylene and the intensity of which increases; (ii) toluene; and (iii) 1,2,4-TMB. Disproportionation products compete with each other (with various adsorption kinetics) and with *o*-xylene for adsorption. The 1,2,4-TMB isomer is strongly adsorbed and is also the fastest to adsorb (as we have seen in Fig. 2). Toluene does not build up so quickly in the pores and stays mainly in the gas phase. Thus, during the first 3 min, toluene is not detected on the surface and 1,2,4-TMB is lacking in the outgoing gas phase. In a second step, after 3-5 min on stream, the yield for disproportionation decreases because the structure is saturated with aromatic rings on Na^+ cations. At the same time, toluene eventually reaches adsorption equilibrium with 1,2,4-TMB, and no further TMB default is measured in the gas phase. In the last step of the reaction, between 1 and 3 h on stream, *m*-xylene progressively adds to the amount of adsorbed xylene, and the intensity of the band at 1482 cm^{-1} still increases.

3.4. Catalytic role of the OH groups

Fig. 5 shows the changes in ν(OH) vibration bands after 1 min or 3 h on reactant stream at 573 K for the whole series of catalysts. Whatever the hydroxyl amount in the sample, only a weak part (high wavenumber component) of the whole infrared ν(OH) signal disappears after 1 min of reaction. When the time on stream is increased from 1 min to 3 h, the amount of consumed hydroxyls increases slightly, but their wavenumber always remains high. Only the most accessible acid sites seem to be efficient for the xylene conversion. We have effectively shown (Table 3) that, at room temperature, only $OH_{unconst}$ are accessible to reactants. OH_{const}

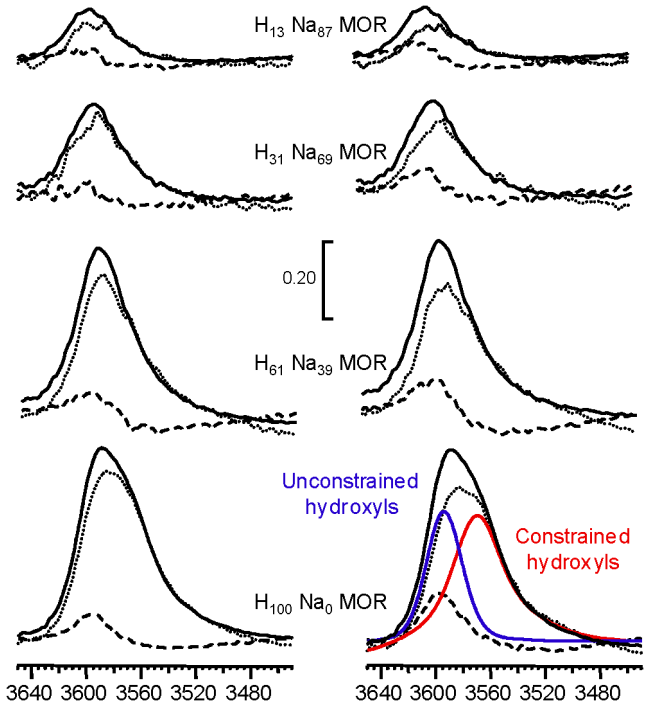

Fig. 5. Infrared spectra in the ν(OH) vibration region for selected $H_xNa_{100-x}MOR$ samples at 573 K: (—) before reaction and (···) after 1 min reaction (left part) or 3 h reaction (right part). Spectra in dotted lines (- - -) correspond to the subtraction between (—) and (···) and represent the hydroxyls consumed during the reaction time. In the bottom right hand corner are superimposed the expected spectra for the $OH_{unconst}$ (high frequency one) and the OH_{const} (low frequency one) at 573 K before reaction which are obtained from the deconvolution procedure described in the text.

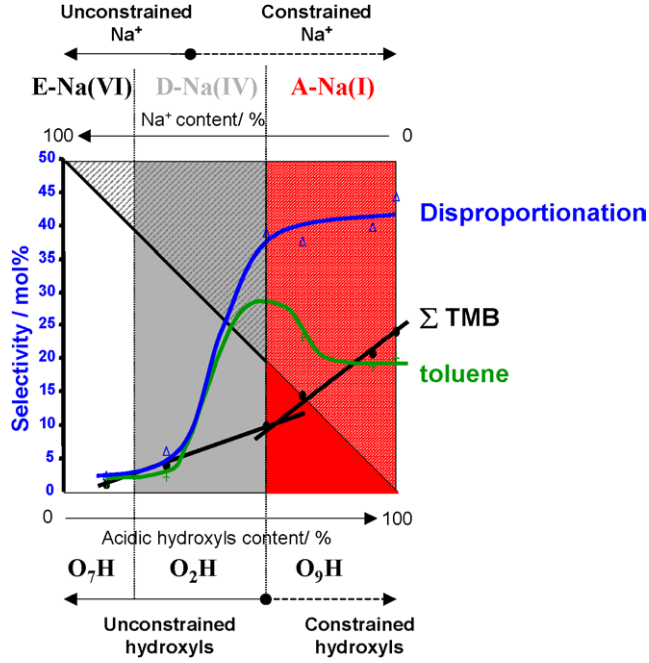

Fig. 6. Evolution of the selectivity in disproportionation products with the acidic hydroxyls content for isoconversion (42%) conditions obtained during the first instants of reaction at 573 K. The denomination of the various hydroxyls and Na^+ cations describes their location and is taken from Ref. [11].

in the side pockets are out of reach for adsorbed species. However, we need to assess this point under reaction conditions at higher temperature. The decomposition of the ν(OH) band into its components at 573 K was carried out according to a procedure described in the literature [15], which was modified as described in the Experimental section to take into account the higher temperature. The decomposition results are summarized in the bottom right corner of Fig. 5. The left peak is relative to the $OH_{unconst}$ (high-frequency) component, and the right peak is relative to the OH_{const} (low-frequency) component. The relative intensities and positions of both components (for $OH_{unconst}$ and OH_{const}) are significantly modified by heating [28], but OH_{const} (signal at lower wavenumber) are never perturbed by any adsorbed species. Even on $H_{100}Na_0MOR$, after 3 h on stream at 573 K, OH_{const}, located at the end of the side pockets, remain out of reach for adsorbed species present on the catalyst. Only $OH_{unconst}$ in the main channels or at the opening of the side pockets are accessible to reactants and can be active in the reaction.

3.5. Compared selectivities

Comparing selectivities for various catalysts in the same reaction is possible only at isoconversion, since the level of secondary reactions is higher as conversion increases. The only published study of this reaction on a series of mordenites with various sodium exchange levels under isoconversion conditions was done with varying temperature [4], but the temperature influences both kinetics and thermodynamics parameters. Fig. 6 shows the results we obtained when working under isoconversion conditions (42% over fresh catalysts measured during the first 3 min of reaction in the presence of a negligible amount of coke) achieved by modification of the space velocities at constant *o*-xylene partial pressure. Selectivity for disproportionation is very low when only a small amount of OH groups is present (in the main channels). It rises significantly above 30% OH groups (30% exchange of Na^+ for H^+), which corresponds to the first O_2H groups appearing at the intermediate position, at the opening of the side pockets, pointing in the main channels [11]. This selectivity increases linearly with the amount of acid sites up to 60%, but then it reaches a plateau and is no longer influenced when OH_{const} groups appear in the side pockets. Therefore, the acidic hydroxyls located on site O_9H (at the end of the site pockets) are not responsible for disproportionation reaction, contrary to what was proposed in the literature [4,7]. This last result is consistent with our observation that OH_{const} are never consumed during catalysis. Considering the distribution in disproportionation products, we observe a continuous increase in TMB selectivity with an exaltation for acidic hydroxyl content higher than 60%. In contrast, the toluene selectivity falls when the last sodium cations are replaced by acidic OH_{const}. Probably because of the cumulative inductive effects of the three methyl groups,

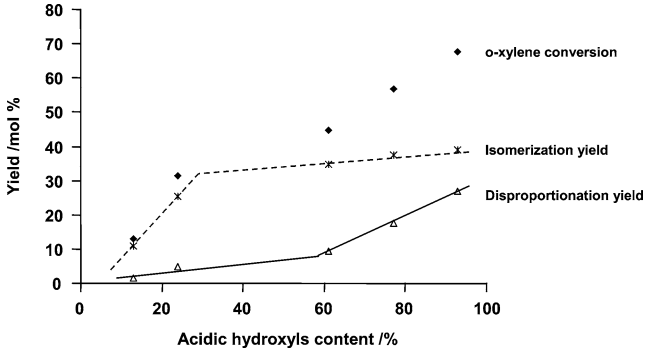

Fig. 7. Evolution of the *o*-xylene conversion together with isomerization and disproportionation yields with the acidic hydroxyls content when the reaction is conduced at constant space velocity (WHSV = 15 h^{-1}) at 623 K. Data reported were obtained after 2 min reaction.

the TMBs are preferentially (and strongly) adsorbed on accessible Na^+ ions, in the main channels or at the opening of the side pockets, whereas toluene becomes the main adsorbed molecule when only acid sites are present. Indeed, as we have seen in Fig. 2, adsorption capacities for TMB and toluene are similar on H_0Na_{100}MOR, whereas the amount of perturbed OH groups in $H_{100}Na_0$MOR is higher upon adsorption of toluene rather than TMB (Table 3).

To summarize, we have clear indications that active sites for disproportionation are the intermediate O_2H groups, located at the opening of the side pockets, whereas O_7H sites in the main channels (when alone) are selective for isomerization. Considering the evolution of the acid strength with cationic exchange, we recently showed that the presence of sodium cations had very little influence on the strength of unconstrained hydroxyls [29]. Moreover, probing the acidity with small molecules such as CO [9,29] or acetonitrile [30] never allowed us to distinguish different signals due to O_7H or O_2H. The acid strengths for these two distinct hydroxyls must then be considered to be similar. The differences in catalytic role are due rather to the larger space made available at the opening of the side pockets when the corresponding cation is removed. When a sodium cation is present at this location, the available space only allows monomolecular isomerization. The increased space after removal of the cation at the opening of the side pockets, together with the induced higher concentration of unconstrained hydroxyls, allows the bimolecular disproportionation to take place. An overall increase in the microporous volume is actually noticed during the exchange process (Table 1), which can account for some of the modifications of the catalyst activity. We report in Fig. 7 the evolution of the initial yields (after 2 min on stream) with the acidic hydroxyl amount (constant space velocity: WHSV = 15 h^{-1} at 623 K). It is obvious from this figure that the overall catalyst initial activity is accentuated for acidic hydroxyl amounts higher than 60%. The initial disproportionation yield increases more than the isomerization yield. This result is consistent with the apparent higher disproportionation selectivity for constrained hydroxyls when no precaution is taken for working under isoconversion conditions. The substitution of the last Na^+ cations on sites A–Na(I) at the end of the side pockets by acidic hydroxyls (O_9H) has a positive effect on the catalyst activity, increasing the space-demanding disproportionation reaction in particular. We previously showed that the acidity of these new constrained acidic hydroxyls (O_9H) was never engaged in catalysis, and, moreover, the replacement of the last Na^+ by these new O_9H does not affect the acid strength of the "working" unconstrained hydroxyls (O_7H and O_2H). We thus propose an indirect effect: (i) the free volume inside the mordenite micropores increases with the ionic replacement of Na^+ by H^+; (ii) when no more Na^+ cations remain the strong interaction with the bulky TMB molecules disappears and the diffusion/desorption of the reaction products becomes easier; and (iii) the space-demanding disproportionation reaction is then favored because of the increase in the overall conversion. These conclusions are only valid for the initial activities (i.e., working with fresh catalysts) because when the time on stream is increased, the void volume inside the micropores is progressively filled by deposited coke [23,29], which influences the reaction selectivities in the same way as adsorbed TMB molecules over Na^+ cations.

4. Conclusions

The first part of this work was devoted to the determination of the infrared bands typical of each product observed during xylene conversion under conditions as close as possible to the reaction conditions. Evaluation of the adsorption capacities in each conversion product for the pure sodium form and the pure acidic form was also undertaken. We managed to give evidence of a strong and fast interaction of the most substituted aromatic ring (TMB) with the Na^+ cations. However, the overall adsorption capacities of 1,2,4-TMB and toluene over H_0Na_{100}MOR are the same under the reaction conditions. On the other hand, toluene is the main adsorbed species at 298 K over the $H_{100}Na_0$MOR containing the highest microporous volume. These preliminary studies enabled us to identify the adsorbed species observed by operando FTIR spectroscopy during the catalytic reaction. Thus we were able to explain the TMB deficit measured during the on-line outlet gas phase analysis for Na^+-containing catalysts: 1,2,4-TMB is preferentially adsorbed during the first instants of reaction, as was shown following the evolution of the surface catalysts during time on stream. Studying the evolution of the consumed hydroxyls when the reaction proceeds, we could then ensure that the constrained hydroxyls located at the end of the side pockets (O_9H) and giving rise to the low-frequency ν(OH) component are never implied in the catalytic act. We then compared under isoconversion conditions the evolution of the selectivities in disproportionation products with the amount of acidic hydroxyls and their localization. We concluded that the first hydroxyls introduced by ionic exchange and located on sites O_7H close to the main channel walls are selective for isomer-

ization (when alone). When the ionic exchange goes on, new acidic hydroxyls are generated on sites O_2H whose presence leads to a selective catalyst in the disproportionation reaction. Heterogeneity in acid strength between O_7H and O_2H was never indicated by basic probe molecule adsorption, so we propose that the high selectivity for the space-demanding disproportionation reaction is due to an increase in the concentration of unconstrained hydroxyls and in the free volume available when the Na^+ cations on site D–Na(IV) are replaced by O_2H. When the last O_9H are created at the end of the side pockets, the isomerization/disproportionation ratio remains constant and only the distribution in disproportionation products is modified, thus producing a modification in the catalyst adsorption properties. Finally, we observed that the initial activity of our mordenite samples strongly increases when "nonworking" unconstrained O_9H are present inside the structure. As they do not participate in the reaction from an acidic point of view, we suggest that their appearance, which corresponds to a strong increase in the microporous volume, favors product diffusion/desorption and as a consequence increases the overall conversion, leading to disproportionation selectivity enhancement.

References

[1] A. Chica, A. Corma, J. Catal. 187 (1999) 167.
[2] G.R. Meima, in: CAT TECH, Baltzer, 1998, p. 5.
[3] T. Terlouw, J.P. Gilson, European Patent 458 378 (1991), to Shell Int. Res. Mij. B. V.
[4] P. Ratnasamy, S. Sivasantar, S. Vishnoi, J. Catal. 428 (1981) 69.
[5] A. Corma, A. Cortes, I. Nebot, F. Tomas, J. Catal. 57 (1979) 444.
[6] A. Martens, J. Perez-Pariente, E. Sastre, A. Corma, P.A. Jacobs, Appl. Catal. 85 (1988) 45.
[7] I. Bankos, A.L. Klyachko, T.R. Brueva, G.I. Kapustin, React. Kinet. Catal. Lett. 30 (2) (1986) 297.
[8] A. Zecchina, L. Marchese, S. Bordiga, C. Pazè, E. Gianotti, J. Phys. Chem. B 101 (1997) 10128.
[9] M. Maache, A. Janin, J.C. Lavalley, E. Benazzi, Zeolites 15 (1995) 507.
[10] F. Geobaldo, C. Lamberti, G. Ricchiardi, S. Bordiga, A. Zecchina, G. Turnes Palomino, C. Otero Arean, J. Phys. Chem. 99 (1995) 11167.
[11] O. Marie, P. Massiani, F. Thibault-Starzyk, J. Phys. Chem. B 108 (2004) 5073.
[12] A. Alberti, Zeolites 19 (1997) 411.
[13] M. Bevilacqua, G. Busca, Catal. Commun. 3 (2002) 497.
[14] J.F. Joly, N. Zanier-Szydlowski, S. Colin, F. Raatz, J. Saussey, J.C. Lavalley, Catal. Today 9 (1991) 31.
[15] M.A. Makarova, A.E. Wilson, B.J. van Liemt, C.M.A.M. Mesters, A.W. de Winter, C. Williams, J. Catal. 172 (1997) 170.
[16] B.M. Weckhuysen, Chem. Comm. 2 (2002) 97.
[17] B. Coughlan, M.A. Keane, J. Chem. Soc. Faraday Trans. 86 (23) (1990) 3961.
[18] B.L. Su, V. Norberg, J.A. Martens, Micropor. Mesopor. Mater. 25 (1998) 151.
[19] S. Chenavarin, F. Thibault-Starzyk, Angewandte Chemie 116 (2004) 1175.
[20] N.S. Nesterenko, F. Thibault-Starzyk, V. Montouillout, V.V. Yuschenko, C. Fernandez, J.P. Gilson, F. Fajula, I.I. Ivanova, Micropor. Mesopor. Mater. 71 (2004) 157.
[21] Selected values of physical and thermodynamic properties of hydrocarbons and related compounds, American Petroleum Institute Project 44, CARNEGIE PRESS, 1953.
[22] A. Corma, E. Sastre, J. Catal. 129 (1991) 177.
[23] F. Moreau, P. Ayrault, N.S. Gnep, S. Lacombe, E. Merlen, M. Guisnet, Micropor. Mesopor. Mater. 51 (2002) 211.
[24] U. Weiß, M. Weihe, M. Hunger, H.G. Karge, J. Weitkamp, Stud. Surf. Sci. Catal. 105 (1997) 973.
[25] N. Arsenova, H. Bludau, W.O. Haag, H.G. Karge, Micropor. Mesopor. Mater. 23 (1998) 1.
[26] M. Guisnet, N.S. Gnep, S. Morin, Micropor. Mesopor. Mater. 35–36 (2000) 47.
[27] A. Vimont, O. Marie, J.P. Gilson, J. Saussey, F. Thibault-Starzyk, J.C. Lavalley, Stud. Surf. Sci. Catal. 126 (1999) 147.
[28] J. Czyzbiewska, F. Thibault-Starzyk, article in preparation.
[29] O. Marie, F. Thibault-Starzyk, P. Massiani, J.C. Lavalley, Stud. Surf. Sci. Catal. 135 (2001) 220.
[30] O. Marie, F. Thibault-Starzyk, J.C. Lavalley, Phys. Chem. Chem. Phys. 2 (2000) 5341.